CHAPTER - 3

DIRECT MEASUREMENTS OF PAIR PRODUCTION CROSS SECTION

3.1 INTRODUCTION

Although very accurate total cross section measurements provide a reasonably precise method of extracting the pair production cross section by making use of accurate theoretical calculations of photoelectric incoherent and cohorent cross sections, the pair production cross section decreases very fast with decreasing energy and at low energy near threshold the method is not suitable for the determination of pair production cross section.

Pair production events may however be separated from scattering and photoelectric effects by detection of two 0.511 Mev photons from the annihilation of the positrons in the target. These come out in opposite directions, since nearly all the positrons are alowed down before annihilation. By placing the target on the line between the two detectors one may detect in coincidence a certain fraction of the total number of annihilation quanta. From a knowledge of the source strength, detection efficiency of the detection system, absorption of incident as well as annihilation quanta and a number of other correction[5], the pair production cross section may be

determined. Many of the experiments of this type overlap both in photon energy and target Z. But the experimental results show wide variation with each other (Table 2.1). The inconsistencies in the measured results must be due to some systematic errors inherent in the measurement which could neither be eliminated nor could be estimated.

For low energy, therefore in order to avoid various systematic errors and uncertainties, it is easier to perform relative measurements to study the screening effects in atomic pair production. That is, in comparison to some standard substance the cross section for the experimental substance can be measured. To find the absolute pair production cross section of the desired element the cross section of the standard element must be known. For low (A) elements screening correction is very small. So, relative to a target element of low Z the cross section for high Z elements can be compared for which screening corrections are important at low energy. But for very low Z elements incoherent pair production, trident production contribute significantly and these are not well known theoretically. Also the counting rates for low Z targets will be very small. So for practical purposes the standard element selected should be of intermediate Z for which the effects of incoherent pair

production and trident production are negligible.

We have therefore made measurements of pair production cross section taking 'copper' as the standard substance for reasons mentioned above.

In order to minimise the response of the detection system to false and accidental coincidences, we have used a coincident circuit having a resolving time of 40 nsec. In the present method various probable sources of errors and uncertainties have been either eliminated or reduced to a minimum by making relative measurements because (a) separate measurements of annihilation pair detection efficiency are not needed (b) total gamma ray absorption coefficient do not enter into the computation of the cross section (c) a large number of corrections to the data are avoided (d) the continuum background does not affect the result and there is no problem in separating the well defined pair annihilation peaks obtained by NaI (Tl) detector.

3.2 Experimental arrangement

The principle of the experimental determination of pair production cross section is simple. Photons of energy greater than threshold for pair production from a source are allowed to strike a target. In the Coulomb field of the target such a photon may disappear producing electron-positron pair. The positron in course of its

passage through the target loses energy and ultimately stops in the target, when it will interact with target electron producing two .511 Mev photons 180^{o} apart. For annihilation in flight slight deviation from 180^{o} is observed. So detection of two .511 Mev photons by two detectors 180^{o} apart in coincidence will ensure the annihilation of a positron and hence a pair production event. A certain fraction of the total number of annihilation quanta thus detected enables the determination of pair production cross section.

3.2.1 Collimation of the gamma ray source

The experimental set up (Fig. 3.1, Table 3.1) has been arranged under rigorous collimation requirements to reduce the background due to pair production in materials other than the target. A uniform conical hole was drilled through a lead cylinder the diameter of the holes being 1 cm at the entry and 1.8 cm at the exit. The cylinder was 16 cm in diameter and 40 cm in length. The source was placed at the entry end and was well surrounded on all sides by lead bricks. There was a minimum of 35 cm lead in any side of the source, allowing only the exit of photons.

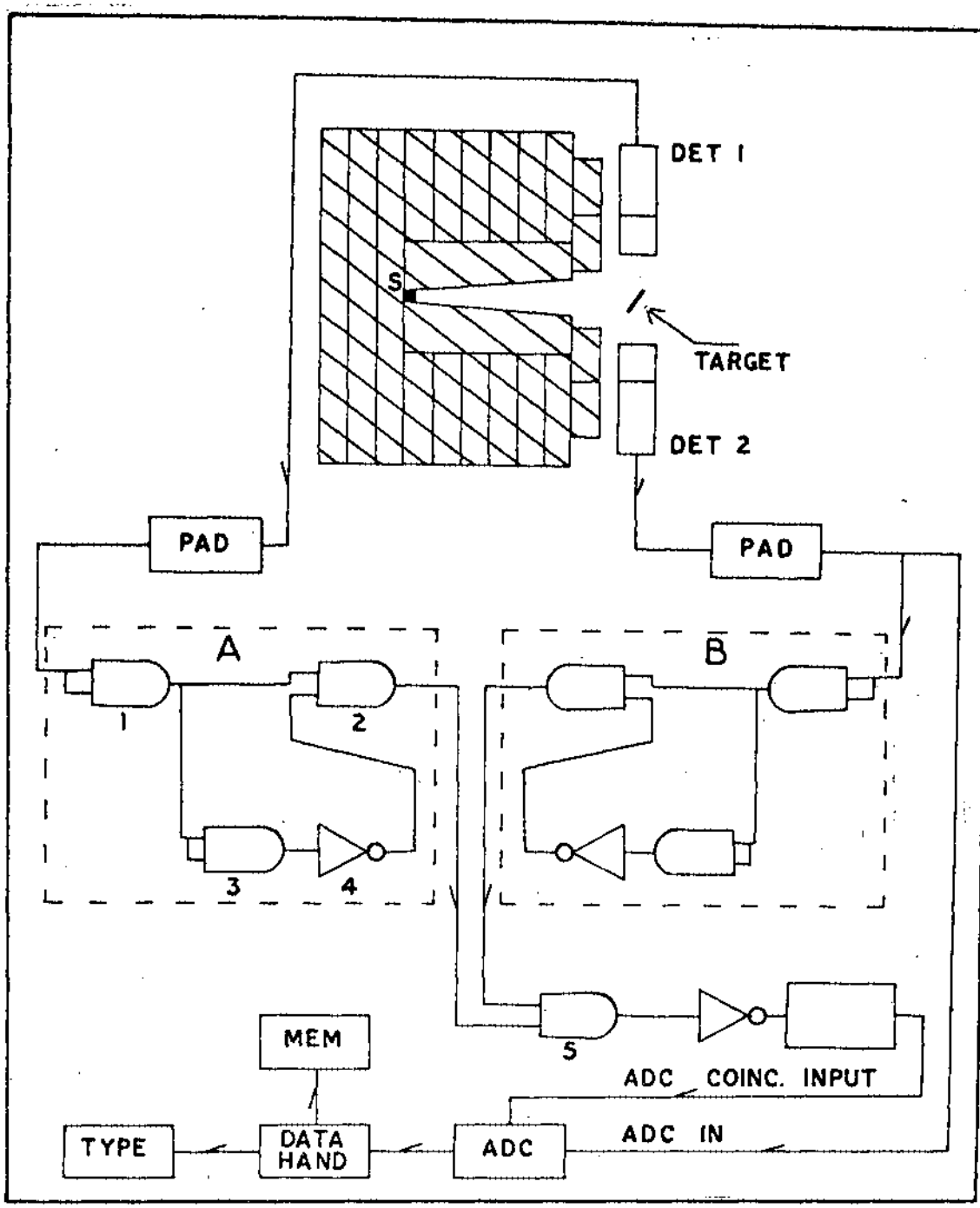

FIG. 3.1. SHOWING THE BLOCK DIAGRAM OF EXPERIMENTAL ARRANGEMENT FOR DETECTING THE ANNIHILATION QUANTA.

Table - 3.1

Basic data of the experimental set up (Fig. 3.1)

1. Source to target distance - 45 cm
2. Source diameter .3 cm for Co^{60} source
   and .8 cm for 65 zn source
3. Detector diameter - 7.5 cm
4. Targets - circular foils of diameter 2 cm.
5. Target to detector distance - 8 cm
6. Solid angle subtend by the detector at the target - 0.69 Sr.

3.2.2 Finite resolving time of the coincidence circuit, chance and accidental coincidences.

Due to finite resolving time of the coincidence circuit the detector system may respond to photons and record a count from events other than annihilation quanta. So an appreciable number of counts recorded by the system may be due to false and chance coincidences. This may introduce an appreciable error in the result of measurements.

This has been minimised by the use of a coincidence circuit having a resolving time of 40 nsec, thus reducing chance and accidental coincidences to a minimum.

3.2.3 Coincidence Circuit

As shown in Fig. 3.1 A and B are two pulse shaping circuits, consisting of three AND Gates and an INVERTER.

The output resulting from the coincidence between the two detectors was used to gate a multichannel analyser (MCA) which recorded the .511 Mev annihilation radiation spectrum from one of the detectors. The gain and biases of the two PADs of the MCA and high voltage supply to each photo multiplier tube of the two detectros (Det-1 and Det-2) were set so that energy calibration of the channels was the same for both detectors. A pulse detected by either of the detectors after being amplified by the respective PADs was fed into two pulse shaping circuits A and B. The amplified pulse from the PAD was applied to the shorted terminals of a dual input AND Gate 1. The output from this gate was applied simultaneously to one input terminal of another dual input AND Gate 2 and to a shorted input terminal of a dual input AND Gate 3. The output from the Gate 3 is inverted by an inverter gate 4 and applied to the other input terminal of AND gate 2. The input logic levels of the input terminals of gate 2 were adjusted so that it gave an output pulse approximately 40 nsec until a pulse from inverter gate 4 changes the logic level therefore whatever be the pulse

width of the output of the PAD, there was always an out put pulse at the output of gate 2 with a width of 40 nsec.

A pulse of similar width was also obtained from the identical circuit for the second detector. These two pulses of width 40 nsec were applied to the in put terminals of a dual input AND gate 5.

So the AND Gate 5 will give an output only when the output pulses from the gate 2 of circuit A and the corresponding one from circuit B arrive within 40 nsec. This output from gate 5 was inverted and applied to the monostable multi-vibrator with schmitt-triger input. The external timing capacitor and resistor were adjusted to obtain a pulse of proper height and width which was applied to the coincidence input of the ADC of MCA. The output pulse of Dectector 2 was fed through the PAD to the ADC input for analysis enabling it to give a pulse spectrum from detector 2 which is in coincidence with detector 1 with a resolving time of 40 nsec.

3.2.4 Positrons formed at the edge or the sides of the target.

Positrons after its formation in the target material are slowed down in the target material and ultimately give rise to annihilation quanta when it

collided with a target electron. But some of the positrons may be formed at the sides of the target and may escape from the target before annihilation. Such an event cannot be recorded and will introduce certain amount of error in the measured cross section.

To eliminate the effect, the target in the form of circular foil was placed inside a perspex holder of cylindrical shape and 1 mm thick in all directions. This thickness was enough to stop all the positrons formed at the sides but thin for annihilation quanta, so the pair formed at the edge of the target will annihilate and will lend itself to be detected by the detection system. The thickness was evaluated from the range energy relationship of the electrons.

3.2.5 Targets

Targets were in the form of thin circular foils of diameter 2 cm. Samples of Copper, Tin, Gold, Thorium and Uranium were 99% pure. Thickness of the foils were in the range .03 - 1.28 gm/cm^2 which was thick enough to stop the positrons, but thin for the incident as well as annihilation photons.

3.2.6 Requirements at the detector system

Since the detector system are designed to detect the .511 Mev photon resulting from the annihilation of

positrons, simultaneous arrival of two .511 Mev photons and detection thereof will ensure a pair event. So the bias and gain of the two detectors were adjusted to be exactly identical with a ^{137}Cs source so that the photo-peaks of ^{137}Cs are exactly at the same channel for both the detectors. The measured resolution of the detectors at ^{137}Cs 662 Mev was 8% at full-width at half maximum of the photopeak.

3.2.7 Gamma Sources

The description of the gamma ray sources used in the measurement are given in table 3.2.

Table - 3.2

Source	Active Size (Approximate)	Physical form	Half life	App. Strength	Energy in Mev
Co-60	3 mm dia x 2 mm long	Sealed Source	5.3 yr	300 mci	1.173 1.332
Zu -65	4 mm dia x 3 mm long	Sealed Source	246 days	100 mci	1.115

3.2.8 Errors arising due to absorption of incident and annihilation photons in the target.

The errors arising from the absorption of incidenct and annihilation photons were taken into account and the effect was eliminated by taking the coincident counts with gradually increased thickness of the target in steps.

For each target element four identical samples were taken. Coincident counts were recorded with one target, two targets, and so on. Thus the number of target atoms were increased in steps. But coincident count rates did not increase proportionately which is due to absorption of incident as well as annihilation photons. Coincident counts were plotted against target thickness the plot is found to fit an equation of the form

$$N_c = Cte^{-Bt} \qquad \ldots (3.1)$$

where C and B are constants, C is the true two photon coincidence count rate for a target of thickness 1 gm cm^{-2}. The targer thickness was determined by taking the mass of the targets and measuring its cross sectional area.

From the observed counts and from a knowledge of the target thickness the values of B and C were determined

by a method of least square

$$\text{Ln}N_c = \text{Ln}C + \text{Ln}t_\gamma - Bt_\gamma \qquad \ldots (3.2)$$

Taking the sum for all the observations

$$\sum \text{Ln}N_c = N\text{Ln}C + \sum \text{Ln}t_\gamma - \sum B t_\gamma \qquad \ldots (3.3)$$

where N is the total number of targets used. Multiplying equation (3.2) by t_γ and taking the sum for all the observations

$$\sum t_\gamma \text{Ln}N_c = \text{Ln}C \sum t_\gamma + \sum t_\gamma \text{Ln}t_\gamma - B\sum t^2 \qquad \ldots (3.4)$$

Multiplying equation (3.3) by $\sum tr^2$ and equation (3.4) by $\sum tr$ respedtively

$$\sum t_\gamma^2 \sum \text{Ln}N_c = N\text{Ln}C \sum t_\gamma^2 + \sum t_\gamma^2 \sum \text{Ln}t_\gamma - B\sum t_\gamma \sum t_\gamma^2 \qquad (3.5)$$

$$\sum t_\gamma \sum t_\gamma \text{Ln}N_c = \text{Ln}C \left(\sum t_\gamma\right)^2 + \sum t_\gamma \sum t_\gamma \text{Ln}t_\gamma - B\sum t_\gamma \sum t_\gamma^2 \qquad (3.6)$$

Substracting equation (3.6) from equation (3.5) we get

$$\sum t_r^2 \sum \text{Ln} N_c - \sum t_r \sum t_r \text{Ln} N_c = N \text{Ln} C \sum t_r^2 + \sum t_r^2 \sum \text{Ln} t_r - \text{Ln} C \left(\sum t_r\right)^2 - \sum t_r \sum t_r \text{Ln} t_r \quad \ldots (3.7)$$

Rearranging we get

$$\text{Ln} C = \frac{\sum t_r^2 \left(\sum \text{Ln} N_c - \text{Ln} t_r\right) - \sum t_r \left(\sum t_r \text{Ln} N_c - \sum t_r \text{Ln} t_r\right)}{N \sum t_r^2 - \left(\sum t_r\right)^2} \quad \ldots (3.8)$$

Hence C

$$C = e^{\frac{\sum t_r^2 \left(\sum \text{Ln} N_c - \sum \text{Ln} t_r\right) - \sum t_r \left(\sum t_r \text{Ln} N_c - \sum t_r \text{Ln} t_r\right)}{N \sum t_r^2 - \left(\sum t_r\right)^2}} \quad \ldots (3.9)$$

In a similar way eliminating C the value of B can be found out and B comes out to be

$$B = \frac{N \left(\sum t_r \text{Ln} N_c - \sum t_r \text{Ln} t_r\right) - \sum t_r \left(\sum \text{Ln} N_c - \sum \text{Ln} t_r\right)}{N \sum t_r^2 - \left(\sum t_r\right)^2} \quad \ldots (3.10)$$

C thus determined from the observed coincident counts by a method of least square gives the true coincident count rate per 1 gm cm^{-2} of the target thickness had there been no absorption of the incident as well as annihilation photons.

3.2.9 Corrections for Compton scattering of the annihilation quanta.

Compton scattering suffered by the annihilation photon may lead to some error in the measured true coincident counts. To keep the spread in the scattering angle to a minimum due to finite size of the scatterer the angle between the plane of the scatterer and the direction of the incident photon beam was found out from the following relation due to Dixon and Storey (Di-68)

$$\frac{r}{R} = \frac{\sin\phi}{\sin(\theta-\phi)} \qquad \ldots (3.11)$$

where ϕ = angle between the plane of the scatterer and direction of incidence and θ is angle between the direction of incident photon and the line joining the detector to the scatterer, r = distance between the target and detector, R = distance between source and target. Values

of r, R, θ and φ are given in Table 3.3.

Table 3.3

Distance between source and target	Distance between target and detector	Angle between the direction of incident photon and line joining the target to detector	Angle between the plane of the scatterer and direction of the incident beam
R (cm)	r (cm)	θ (degree)	φ (degree)
40	8	90	11.3

3.2.10 Reduction of Background counts

To minimise the effect of false and chance coincidences the two detectors were covered with 2 cm Pb cylinder. This shielding reduced the background from external sources considerably. The background readings were taken with the two detectors at 180° positron as well as in 90° position with the holder in position and

holder removed and the source in position. The background at 180° position of the detectors was 2520 counts in 40 K sec without holder in position and 2496 counts at 90° position of the detectors.

Background with holder removed and source in position was found to be exactly identical at 180° and at 90° position which was taken as the background due to false and accidental coincidences. Nearly identical readings in the two cases ensured constancy of the background.

3.2.11 Small angle scattering of annihilation photons.

Scattering of any of the pair annihilation photons may prevent the photon from reaching the detector and thus may escape detection if the solid-angle subtended by the detector at the position of the scatterer is small. This effect was taken into account by placing the two detectors exactly at a distance of 8 cm from the centre of the target. Thus keeping the solid angle to a reasonably high value. The error arising out of scattering was thus reduced to a minimum.

3.3 Experimental procedure and measurements.

If C be the true coincident counts per gm cm^{-2} when a target of atomic number Z is exposed to gamma

-ray beam of intensity Φ placed at a distance R from the target then it can be considered to the pair production cross section by the following relation.

$$C = \frac{\Phi}{4\pi R^2} \frac{N_0}{A} \epsilon \sigma \qquad \ldots (3.12)$$

where N_0 is the avagadro's number, ϵ is the efficiency of detection of the pair production cross section per atom of the material of the target, and A the atomic weight of the target material. In order to determine σ other unknown quantities has to be measured as for example Q, R and ϵ . Determination of Φ and ϵ -leads to uncertainty in the measurements and so will give rise to some error in the measured result. Some sort of systematic errors are likely in the determination of these unknown quantities and these are very difficult to eliminate completely. We have therefore avoided the determination of these factors.

By observing the two annihilation quanta at 180° apart created in a target "X" of atomic number Z the spectrum of annihilation photons at the given direction with respect to the incident photon beam was recorded along with an exactly similar lower Z comparison radiator placed at the same positions of "X" in exactly same

geometry. Counting time was adjusted to give reasonably good statistics. As screening correction is small in low Z elements at low energy the standard element should be a low Z material.

If C_x and C_{cu} be the true coincidence counts as determined experimentally this procedure gives for the cross section ratio from equation (3.12)

$$\frac{\sigma_x}{\sigma_{cu}} = \frac{C_x A_x}{C_{cu} A_{cu}} \qquad \ldots (3.13)$$

where σ_x and σ_{cu} are the cross sections for the pair production of the target "X" having an atomic weight Ax and σ_{cu} and A_{cu} are the corresponding quantities for copper, respectively.

3.3.1 Procedure

The source target assembly was placed as shown in fig. 3.1 , the connecting leads from the detector to the multichannel analyser kept at 20°C was made of exactly equal lengths so that there was no time delay introduced due to unequal length of the leads. The detection system was 7.5 cm x 7.5 NaI (Tl) mounted on 8054 photo multiplier. The detector system was then calibrated

in such a way that photopeak of .511 Key gamma rays from 22 Na source was exactly at the same channel for the two detectors by adjusting the gain and bias of the two detectors. Several weak gamma ray sources were used for the purpose. These settings were checked at least once in every 24 hours and no detectable drift of the photopeak was observed.

During measurement with each sample position of the photopeak with 22 Na source was checked and rechecked against any fluctuation. A holder made of perspex was used to place the target in position.

To minimise the effect of background (chance and false coincidences) resulting from interactions other than pair production in the target and short term variation of detection efficiency of annihilation photons, the data were taken alternatively on each set of standard and sample targets in the following sequence: Standard target (coincidence rate at 180^{o} and at 90^{o} between the axes of the two detectors), sample targets (coincidence rate at 180^{o} and 90^{o} position of the two detectors), background coincidences (with and without holder) at the two positions, standard target and so on. The 'sample' and 'standard' target coincidence rates at the 90^{o} position were taken as the chance coincidence rate

in the determination of pair annihilation coincidence rate at 180° position and have been used to correct the observed coincidence spectrum. Counting times from 40 K ksec to 100 K sec were used. The measurements were carried out at an ambient temperature of 20°C and it was maintained constant throughout the period of the measurement. For experiment with Co-60 source all the 512 channels were used for storing the data, and only 256 channels were used for experiment with Zn-65 source.

3.3.2 Errors and Correction

The various sources of errors taken into consideration in the analysis of the data are discussed in this section.

(a) Uncertainty in the determination of the area of the annihilation spectra.

The raw data after subtraction of the background were fed to the microcomputer 1101 of DCM and fitted to a gaussian. Fitted spectra along with raw annihilation spectra are shown in Fig. 3.2 - 3.9.

It is very clear from the figures that in the present experimental set up and the detection system used there was no difficulty in separating the well defined .511 Mev spectra resulting from the annihilation of positrons. Total counts were obtained by evaluating

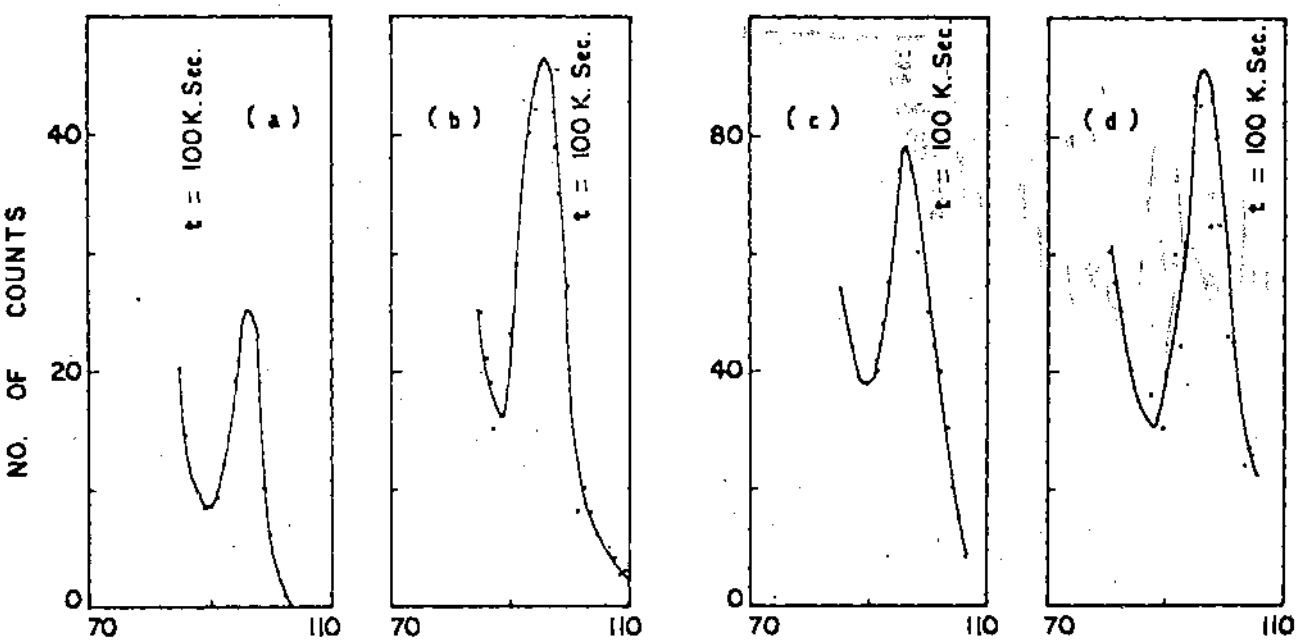

FIG. 3.2. ANNIHILATION SPECTRA FOR COPPER WITH ^{65}Zn -SOURCE.
a, b, c and d CORRESPONDS TO INCREASING TARGET THICKNESS.

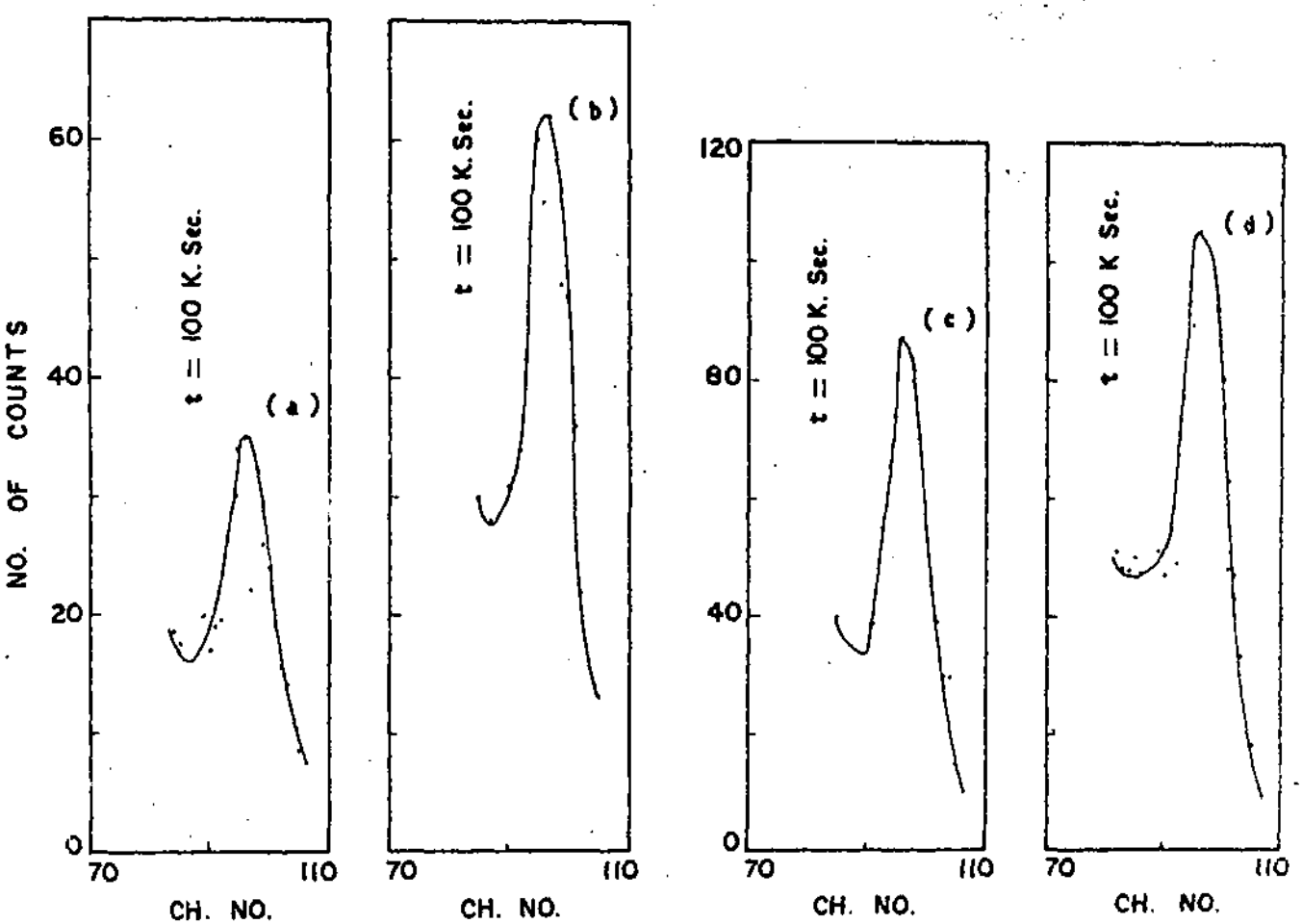

FIG. 3.3. SAME AS FIG. 3.2 BUT FOR TIN.

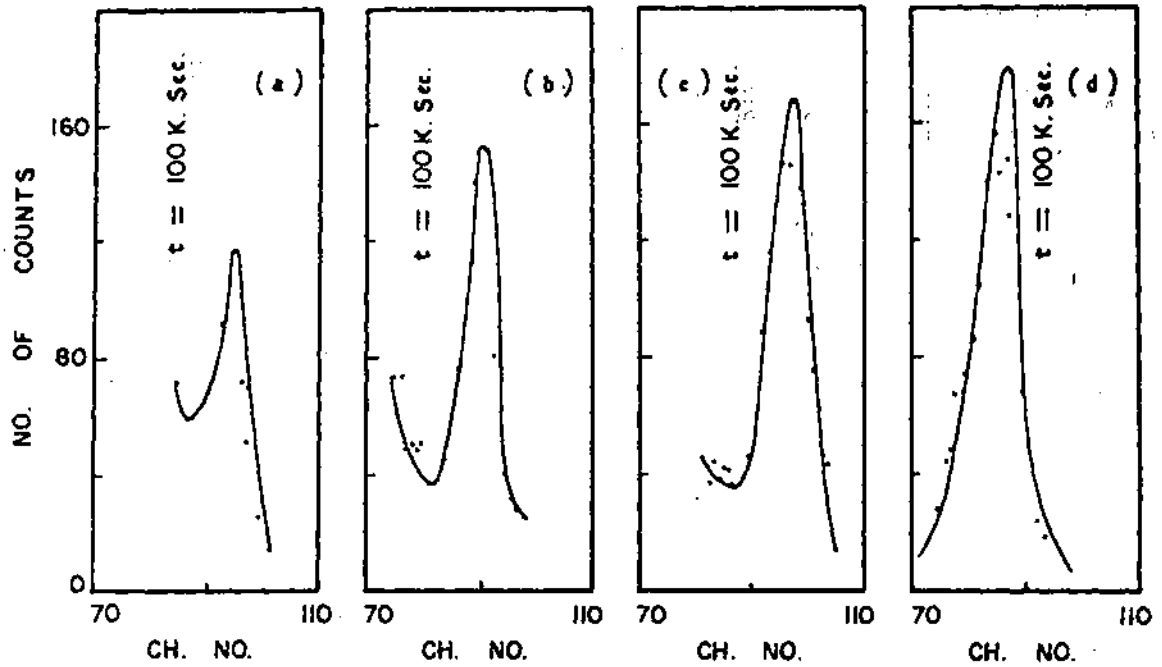

FIG. 3.4. ANNIHILATION SPECTRA FOR GOLD WITH ^{65}Zn SOURCE.

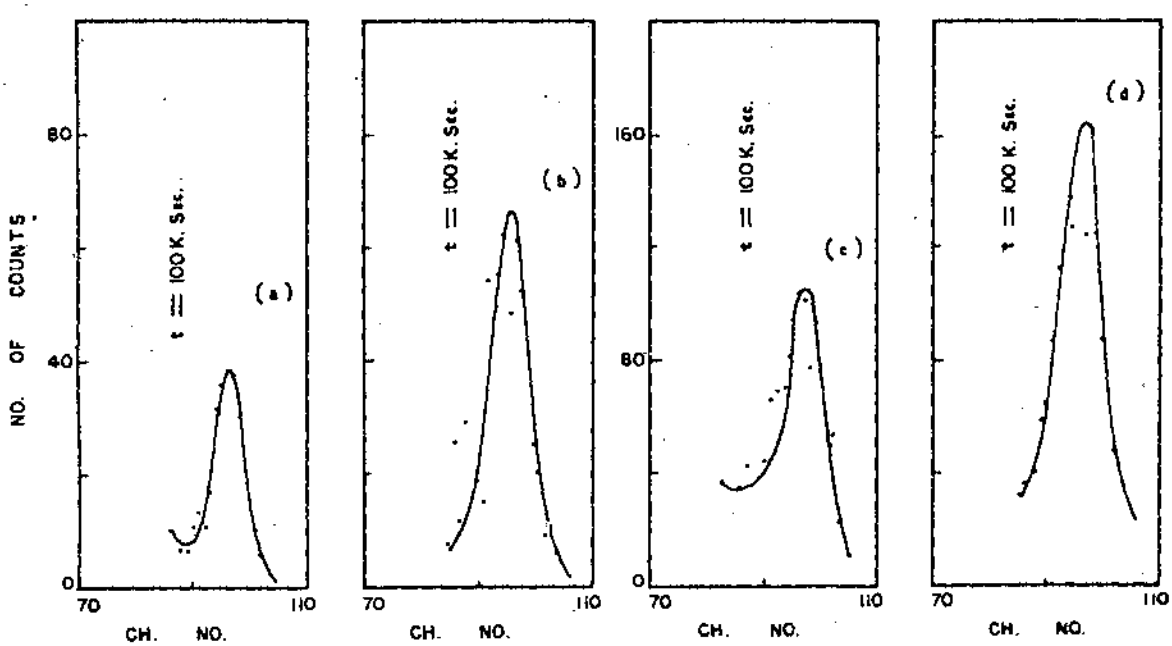

FIG. 3.5. SAME AS FIG. 3.4 BUT FOR THORIUM.

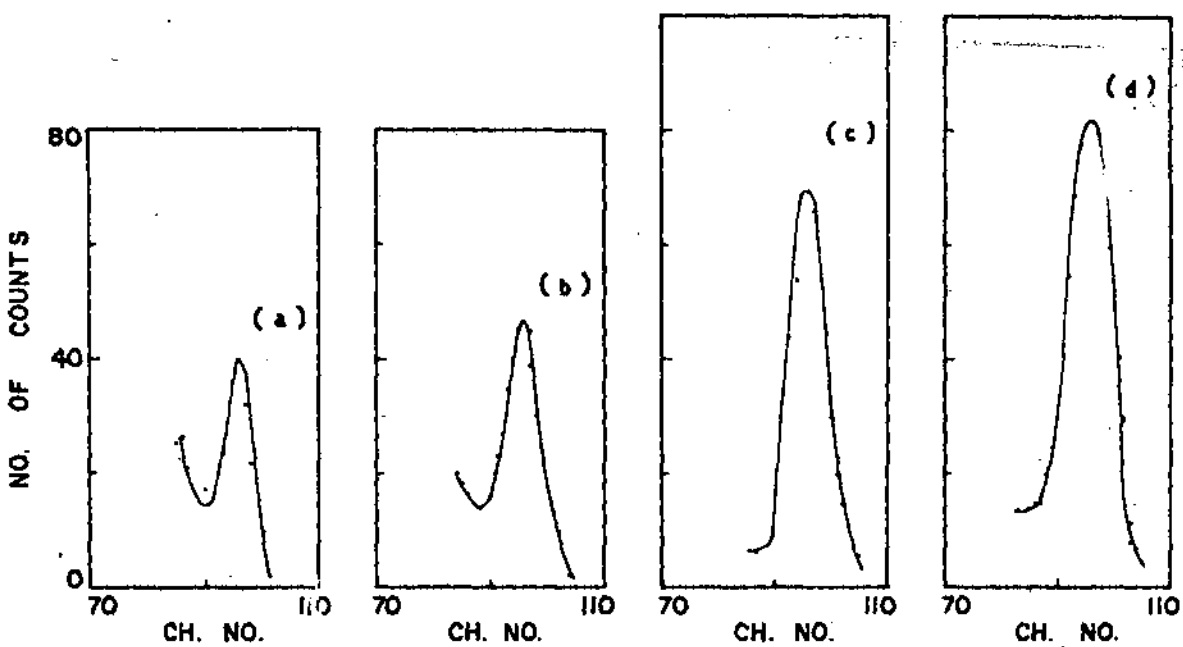

FIG. 3.6. SAME AS FIG. 3.2 BUT FOR URANIUM.

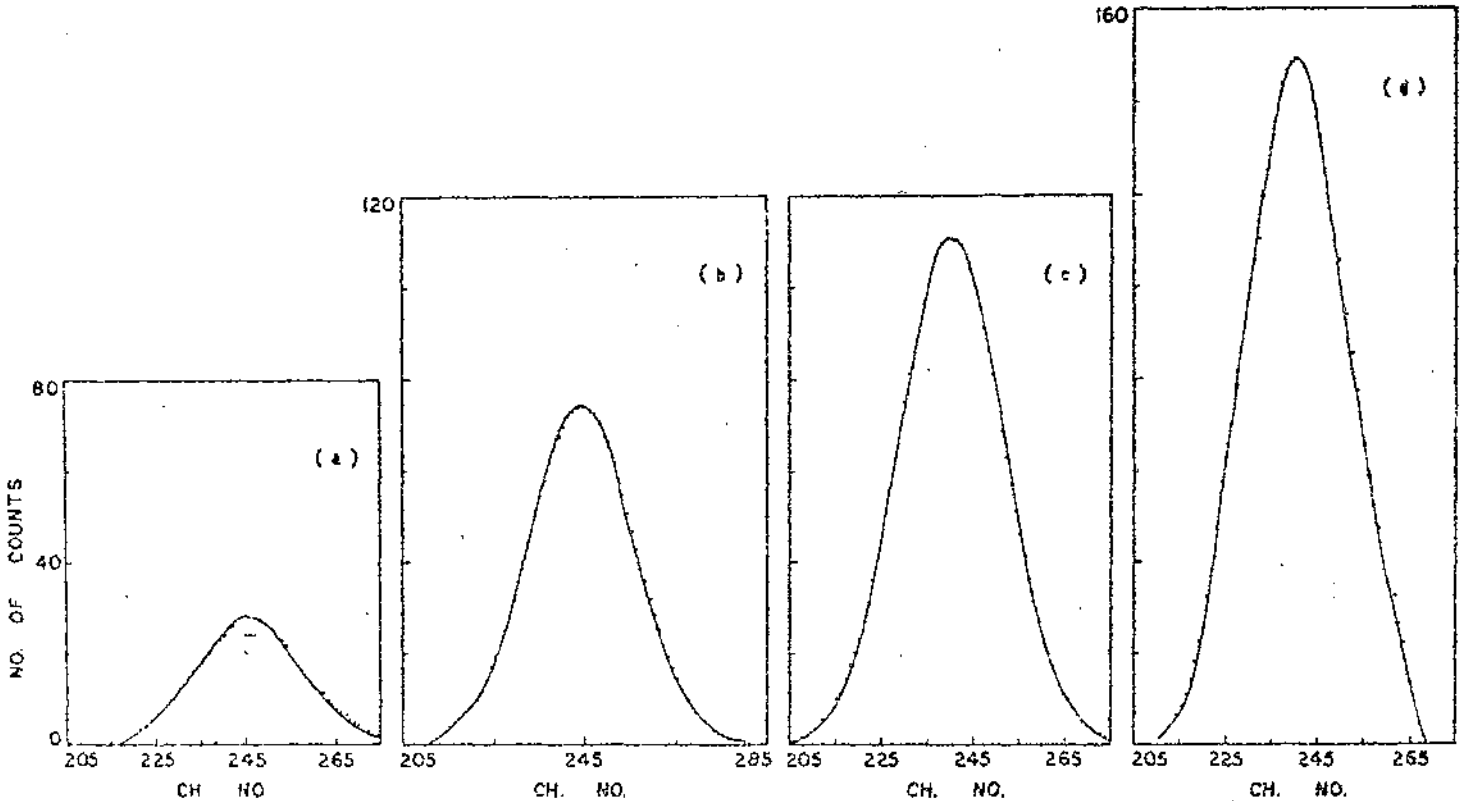

FIG. 3.7 ANNIHILATION SPECTRA FOR COPPER WITH ^{60}Co - SOURCE. GRAPHS a, b, c and d CORRESPONDS TO INCREASING TARGET THICKNESS.

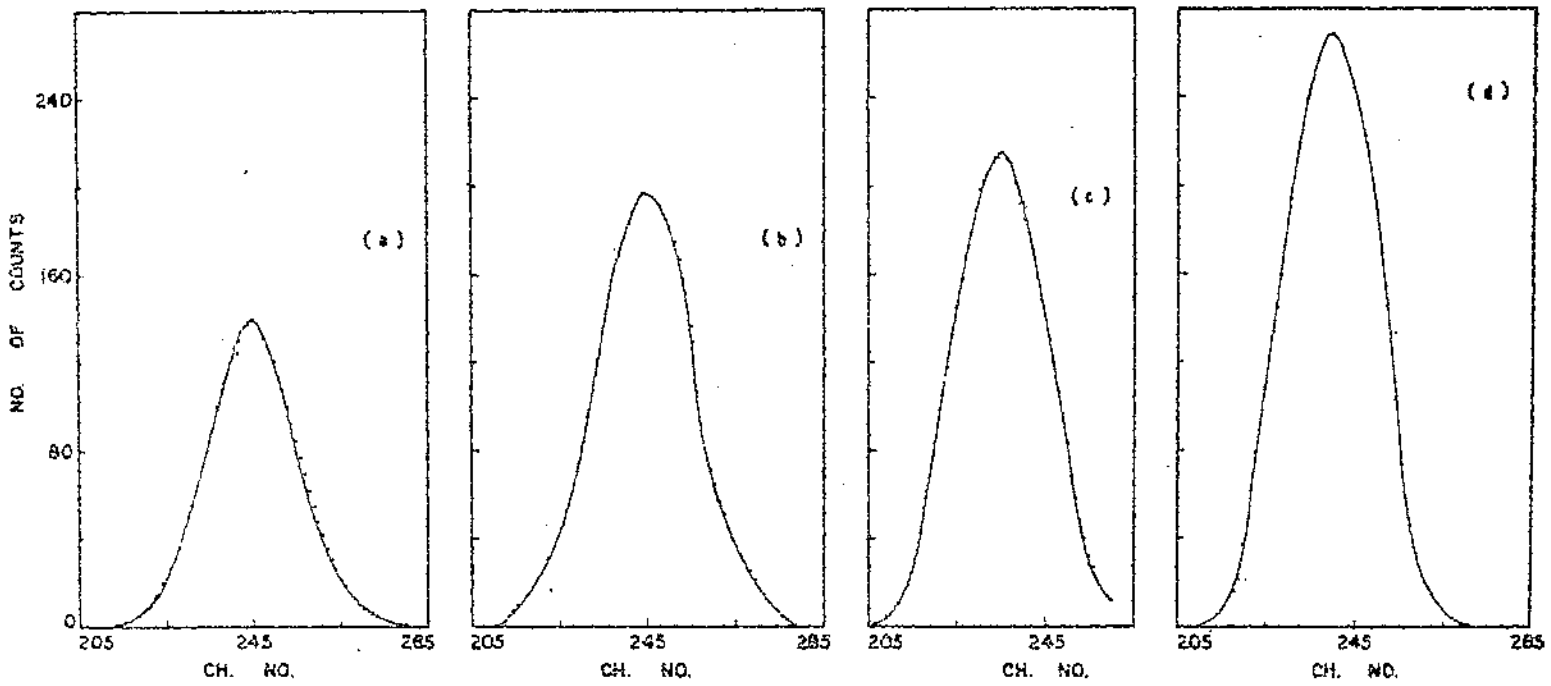

FIG. 3.8. SAME AS FIG. 3.7 BUT FOR TIN.

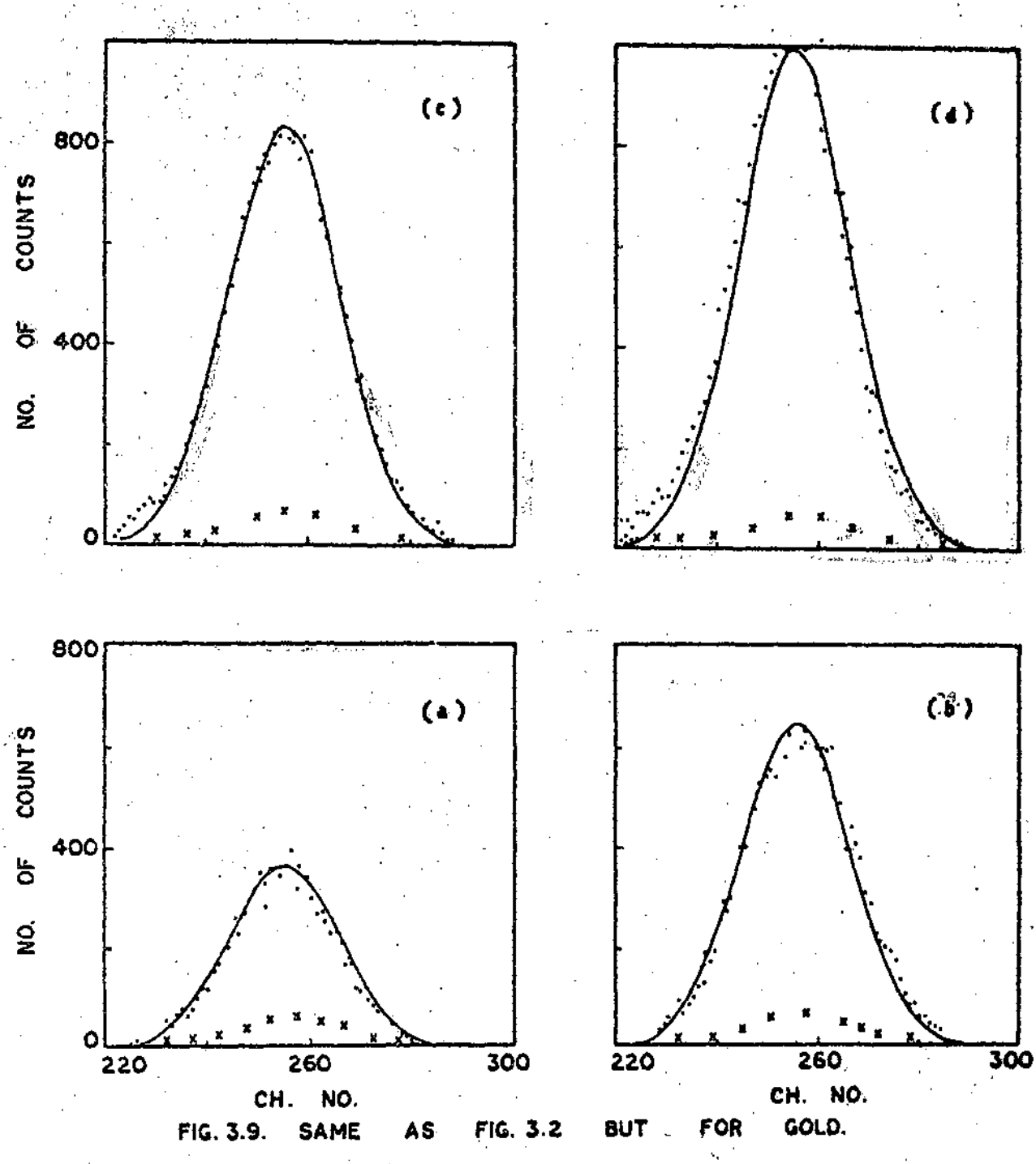

FIG. 3.9. SAME AS FIG. 3.2 BUT FOR GOLD.

the photopeak area by using the formula (3.14)

$$A = H b_{\frac{1}{2}} \left(\pi / 4 \log_e 2\right)^{1/2} \quad \ldots (3.14)$$

where H is the maximum peak ordinate and $b_{\frac{1}{2}}$ is full width at half maximum of the photopeak for a gaussian. Also the total counts in a photopeak was determined through simple addition of the counts in the single channels under photopeak. The results of the two evaluation are found to agree within 1 percent.

(b) Statistical errors

Statistical errors of a measurement of the intensity of the annihilation spectra has been expressed by standard deviation in the total number of annihilation counts. For measurement with ^{60}Co source this was 3.62% and for measurement with ^{65}Zn source this was 2.7%.

(c) Corrections for the decay of the source

The decay correction for the period of the experiment was evaluated by recording the decay curve.

Relative Activity $A_0\lambda / A\lambda$ or relative amounts of radioactive nuclides are plotted on a semilogarithmic axis against time on the linear scale, then $e^{-\lambda t}$ is a straight

line passing through the points $A/A_0 = 1$ at $t = 0$ and $A/A_0 = .5$ at $t = T$ where T is the half life of the source. From which activity at any time can be evaluated to a high degree of accuracy in term of the initial activity.

(d) Errors due to finite energy resolution of the detectors.

Since we have taken the area ratio of annihilation peaks the finite energy resolution of the detectors did not affect this ratio.

(e) Error in the determination of efficiency of the detectors and Geometry factor.

Any error in the determination of efficiency of the detectors does not enter because this factor and effective solid angle factor cancel out in the measured ration.

(f) Determination of activity of the primary source did not enter into our computation of the area ratio of photopeaks.

(g) Errors due to absorption of primary as well as annihilated photon.

As has already been explained in section 3.2.8 the effect of absorption was taken into account and corrected for recording the annihilation spectra with

gradually increasing thickness for each sample. Corrected true coincidence counts were obtained by a method of least square fit as explained there.

3.4 Results:

Pair production cross section ratio data was obtained from measurements made at a solid angle of 0.87 Sr between the target and detector. The sample thickness was determined to an accuracy of .05%. Coincidence countrate as obtained from the measured area of the annihilation spectra fig. 3.2 - 3.9 has been plotted against target thickness fig. 3.10 - 3.17 . The resulting curve is found to fit an equation of the form

$$N_c = Cte^{-Bt}$$

where C and B are constants C is the true coincidence count if there had been no absorption of the incident and annihilation photons C and were determined by a method of least square fit for each target material and for each energy. Evaluation of C leads to the determination of cross section ratio from a knowledge of the Atomic weight of the target material.

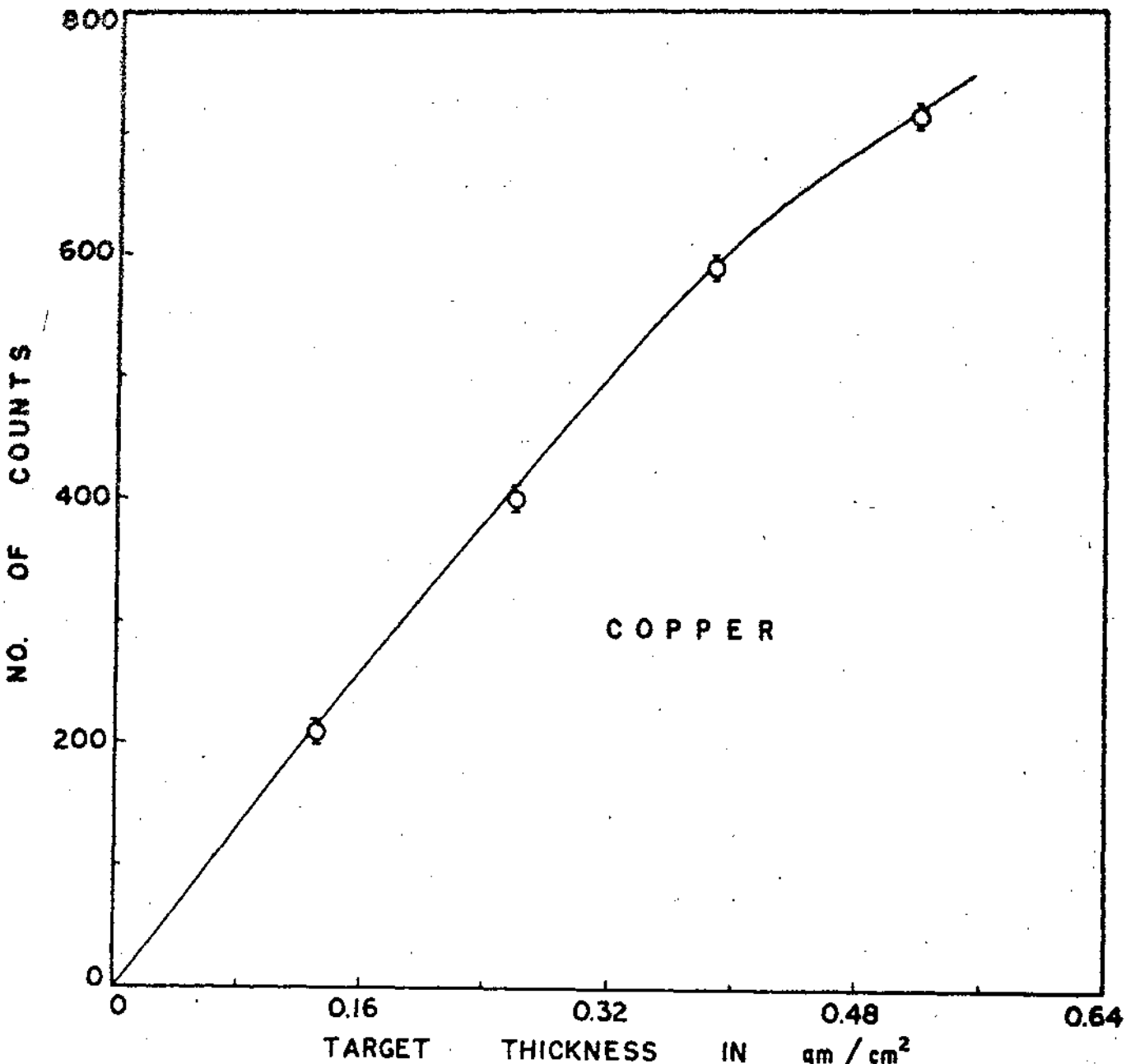

FIG. 3.10. OBSERBED COUNTS VS TARGET THICK-NESS WITH Zn – 65 SOURCE AND COPPER TARGET.

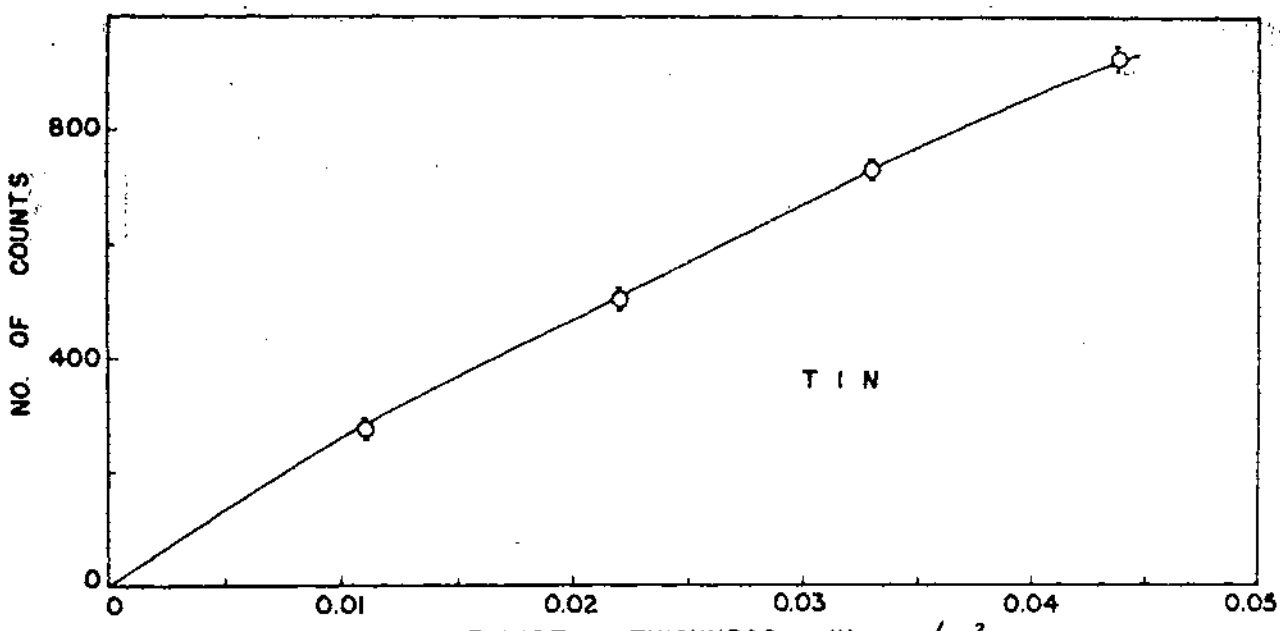

FIG. 3.11. SAME AS IN FIG. 3.10 BUT FOR TIN

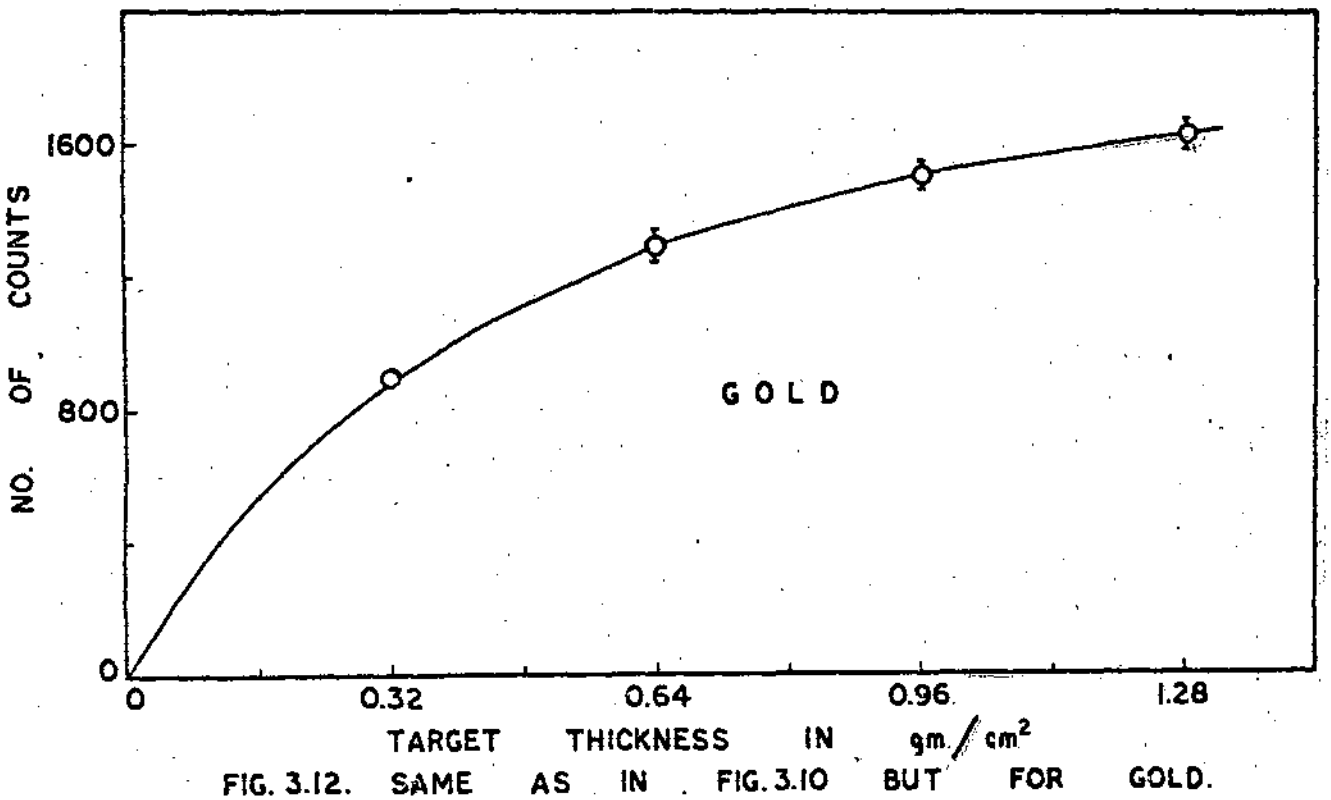

FIG. 3.12. SAME AS IN FIG. 3.10 BUT FOR GOLD.

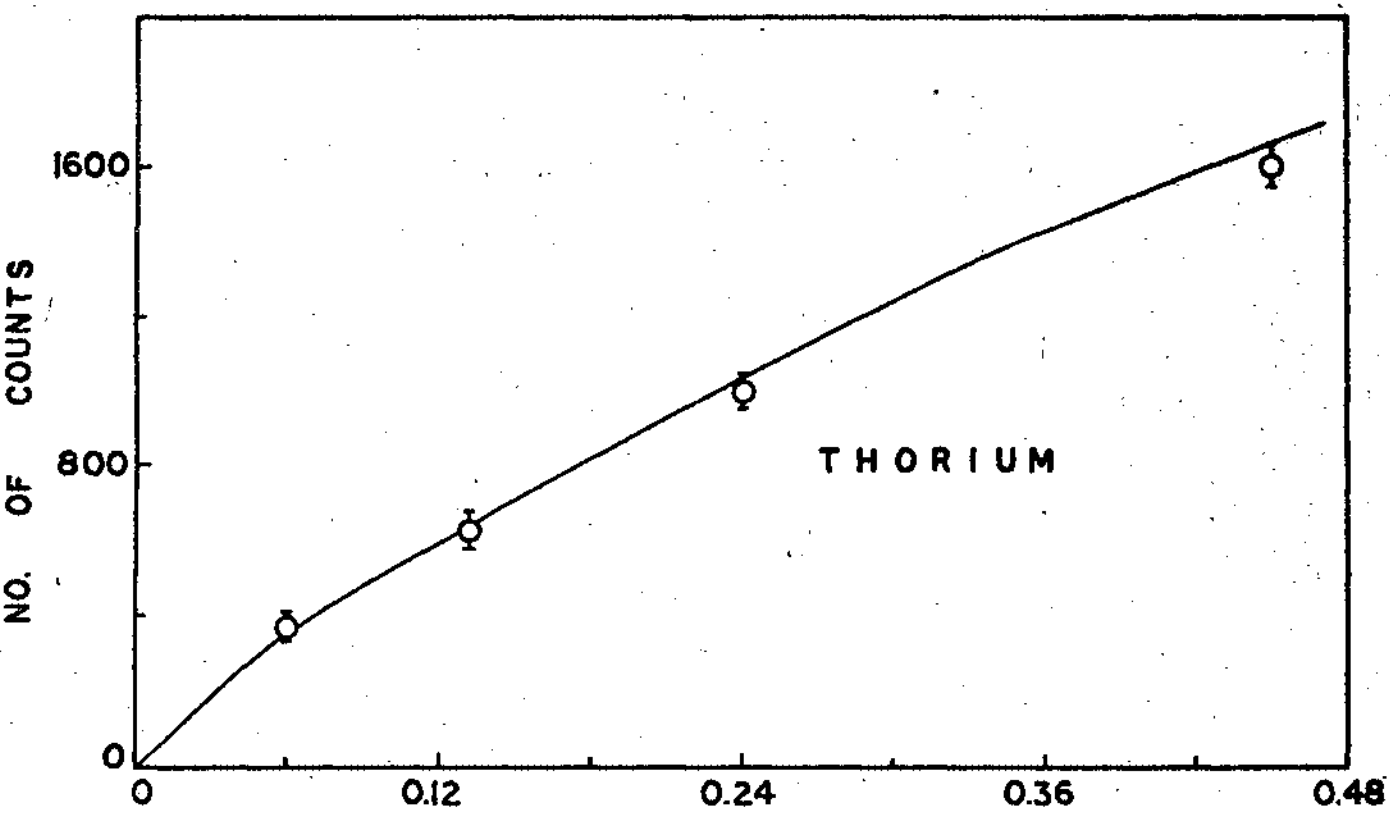

FIG. 3.13. SAME AS IN FIG. 3.10 BUT FOR THORIUM.

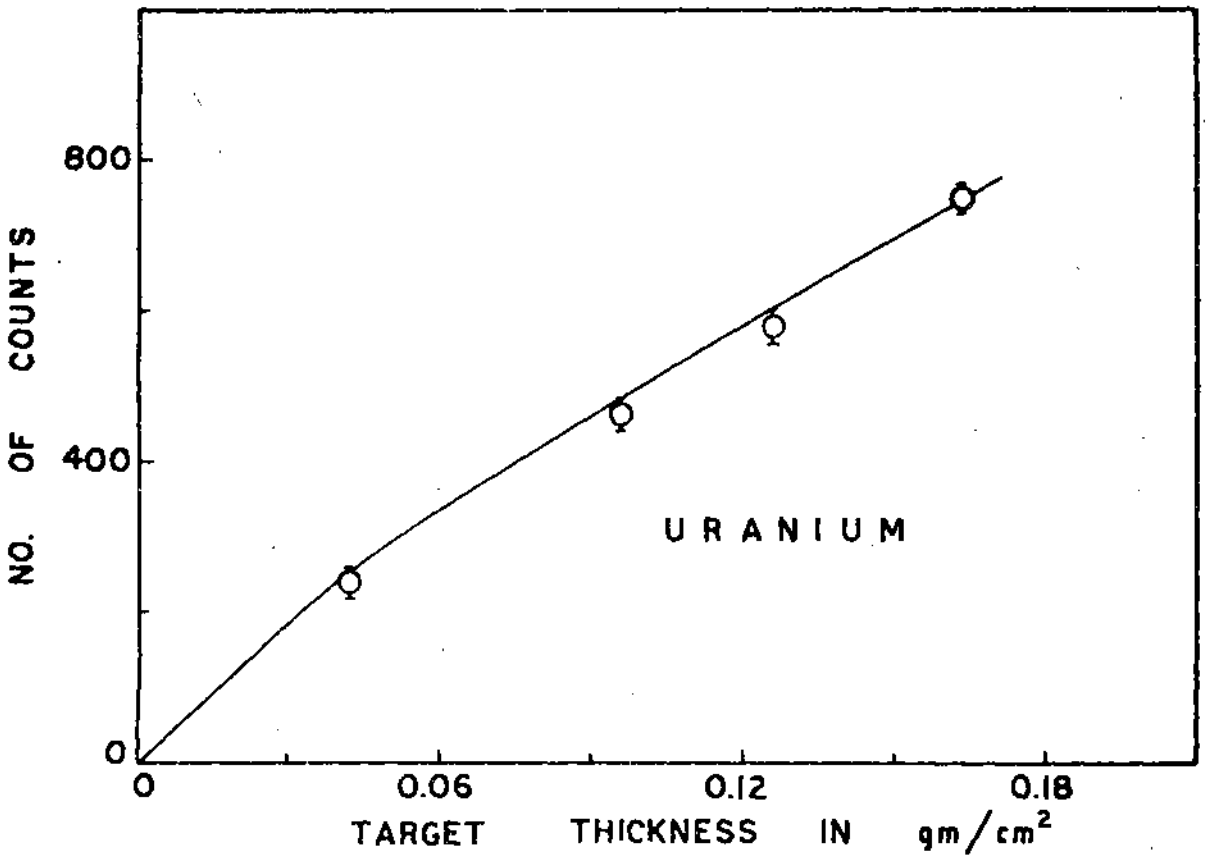

FIG. 3.14. SAME AS IN FIG. 3.10 BUT FOR URANIUM.

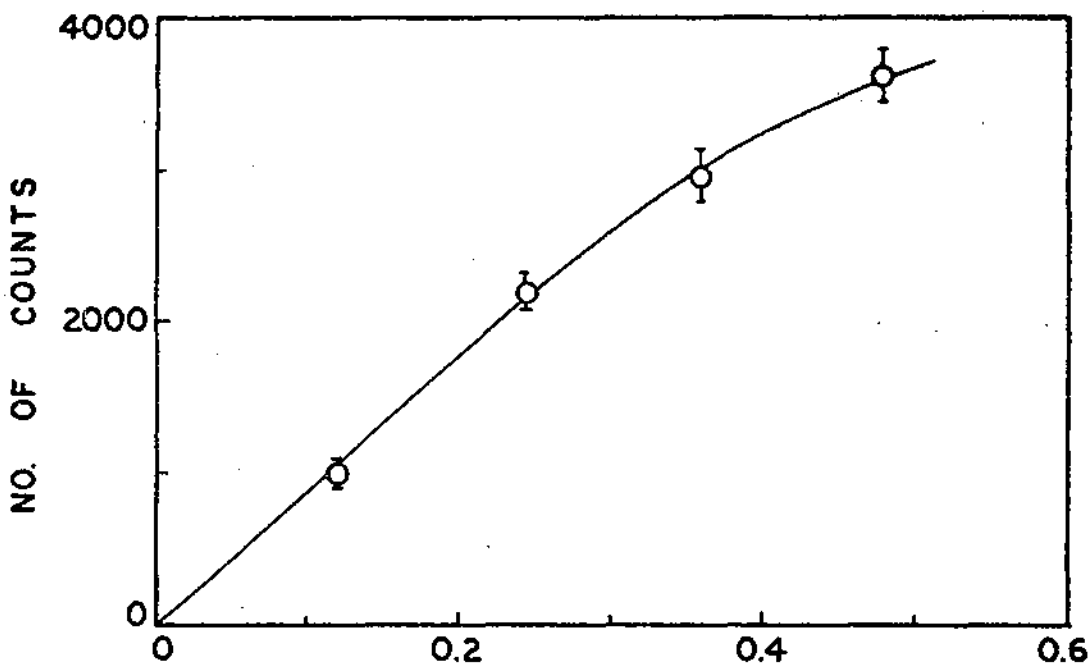

FIG. 3.15. OBSERBED TOTAL COUNTS PLOTED AGAINST TARGET THICKNESS (Gms. Cm^{-2}) FOR COPPER WITH CO – 60 SOURCE.

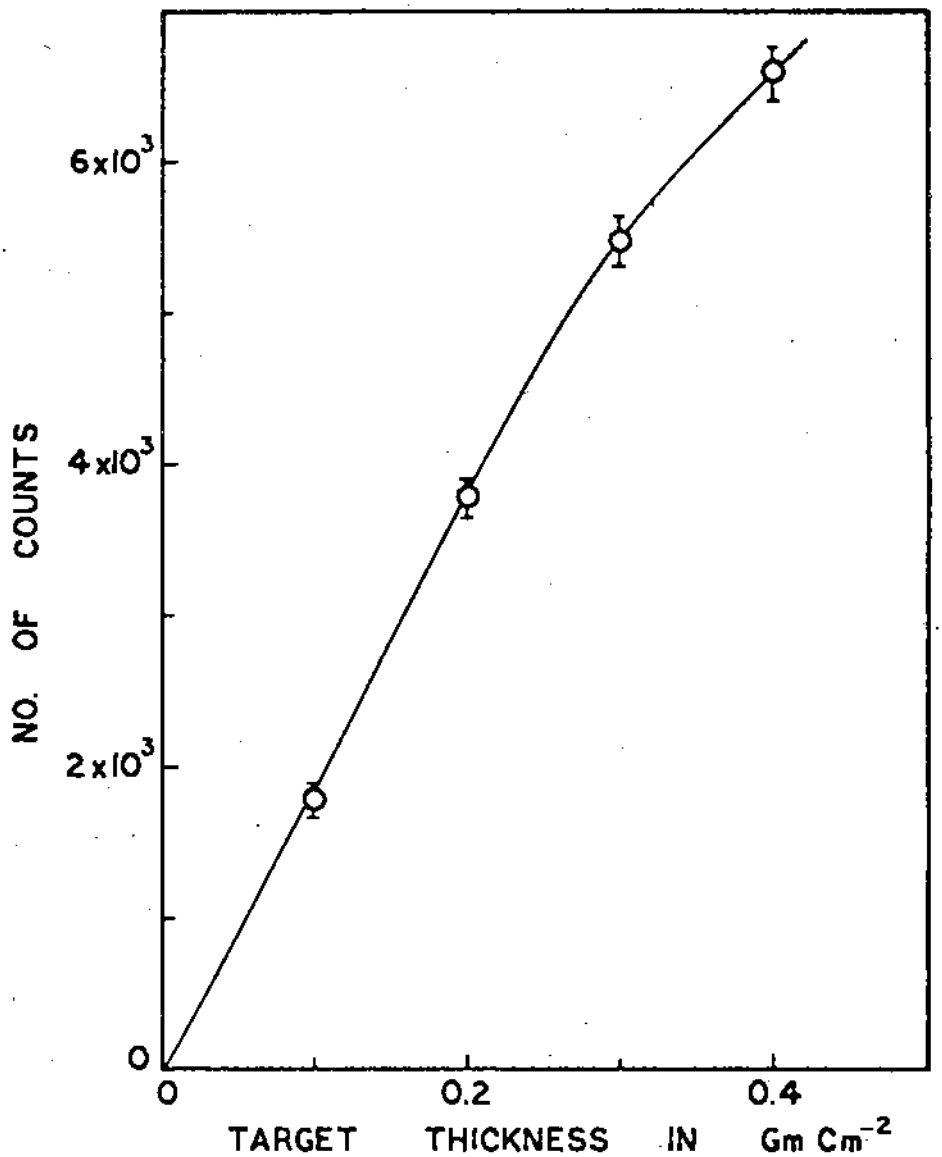

FIG. 3.16. SAME AS IN FIG. 3.15 BUT FOR TIN WITH CO – 60 SOURCE.

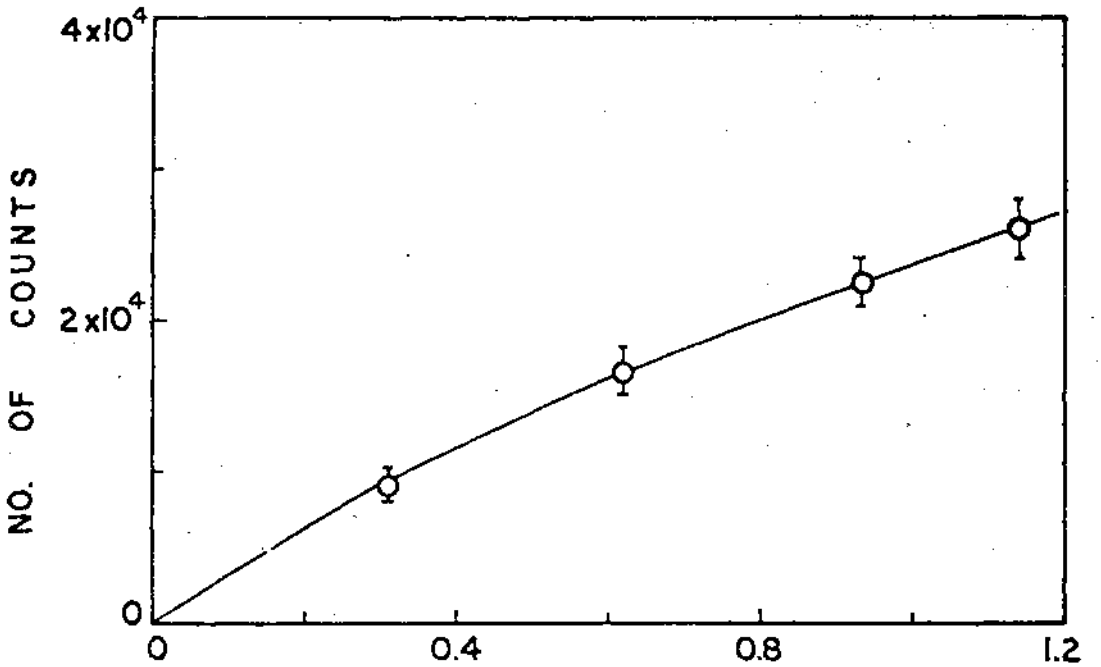

FIG. 3.17. SAME AS FIG. 3.15 BUT FOR GOLD WITH CO - 60 SOURCE.

Cross section ratios are shown in Table 3.4 along with some other experimental results. From the measured ratio absolute cross sections have been evaluated with the help of accurate theoretical cross section for copper for which screening correction is very small and the results are shown in Table 3.5 and Table 3.6. The cross section ratios are shown in Figs. 3.18 - 3.19 along with other recent measurements and latest theoretical calculations.

3.5 Discussion

The effect of screening on the cross section of pair production near threshold is important for atoms of larger atomic number. As demonstrated in Fig. 3.18 and 3.19 where results of σ_z/σ_{Cu} have been plotted against atomic number from different theoretical calculations and direct measurements along with the present experiments, it is easier to check experimentally the screening correction in the presently adopted method that avoids various sources of errors which were found to be very difficult to remove in earlier direct experiments (Av-14, Gi-78,79). Most of the recent experiments used Ge (Li) detectors which give a lower counting efficiency resulting in poor statistics.

The results of the present set of measurements thus demonstrated the suitability of the present method, in making direct experimental check on the screening correction for pair production cross section at energies near threshold.

Table - 3.4

Theoretical and Experimental cross section ratios

Energy in Mev	Ratio	THEORETICAL				EXPERIMENTAL					
		Born approxi-mation	Øverbo PC	Øverbo SC	Tseng Pratt SC	Girard et al	Dayton	Standil et al	Schmidt	Henry et al	Present expt.
1.332	σ_{Sn}/σ_{W}	2.97	3.83	3.95	3.93	3.85	3.66	3.48	3.47		3.97 ±.15
1.173	σ_{Au}/σ_{W}	7.40	12.74	14.00	13.68						14.14 ±.33
	σ_{Pb}/σ_{W}	7.99	13.86	15.56	15.12	15.33 ±0.92	14.70	13.93	13.69	15.29 ±.33	
	σ_{U}/σ_{W}	10.07		21.52	20.79	21.4 ±1.32					
	σ_{Sn}/σ_{W}	2.97	3.335	3.589	3.64						3.77 ±.20

Contd..

Table - 3.4 (Contd..)

Energy in Mev	Ratio	THEORETICAL				EXPERIMENTAL					
		Born approxi-mation	Øverbo PC	Øverbo Sc	Tseng Pratt SC	Girard et al	Dayton	Standil et al	Schmidt	Henry et al	Present expt.
1.115	σ_{Au}/σ_{Cu}	7.42	6.38	10.58	8.99						10.53 ±.71
	σ_{Th}/σ_{Cu}	9.62	6.81	14.41	11.01						12.4 ±.97
	σ_{U}/σ_{Cu}	10.06	6.83	15.66	11.38						13.18 ±1.04

Theoretical and Experimental pair production cross section in mb/atom

Energy in Mev	Element Z	σ_B	$\sigma_{Pc}^{\phi o}$	$\sigma_{Sc}^{\phi o}$	σ_{Sc}^{TP}	Present experimental taking cross section value of copper		Other Experiments			
						10.1 from ϕo.-79	10.00 from Ts.-72	1	2	3	4
	50	24.03	38.20	39.90	39.50	40.17 ±1.54	39.70 ±1.54	32.68	40.5 ±2	35.9	33.16
	79	59.82	126.83	141.40	136.83	142.71 ±3.22	141.30 ±3.22				
1.332	82	64.66	137.7	157.2	151.2				161±6		
+ 1.173	92	81.36		217.3	207.00				222±9		

σ_B - Born approximation cross section
$\sigma_{Pc}^{\phi o}$ - Øverbo point coulomb calculation ref (ϕo-67)
$\sigma_{Sc}^{\phi o}$ - Øverbo screening corrected calculation ref. (ϕo-79)
σ_{TP}^{Sc} - Tseng Pratt screening corrected calculation (Ts-72)

1. P.Schmidt and P.Hubber (Sc-54)
2. Girard et al - (Gi-78,79)
3. I.F.Dayton - (Da -53)
4. S.Standil and V.Shkolnik (St-58)

Table - 3.6

Theoretical and experimental pair production cross section in b/atom

Enefgy in Mev	Element Atomic number	σ_B	$\sigma_{Pc}^{\phi o}$	$\sigma_{Sc}^{\phi o}$	$\sigma_{Sc\ TP}^{TP}$	Present experimental taking the cross section of copper as 9.64×10^{-4} from (a)	Present experimental taking the cross section of copper as 9.63×10^{-3} from (b)
	50	1.895×10^{-3}	3.017×10^{-3}	3.460×10^{-3}	3.520×10^{-3}	$(3,634 \pm .019) \times 10^{-3}$	$(3.630 \pm .019) \times 10^{-3}$
	89	4.733×10^{-3}	5.774×10^{-3}	1.02×10^{-2}	8.660×10^{-3}	$.010 \pm .00068$	$.0101 \pm .00068$
1.115	90	6.142×10^{-3}	6.16×10^{-3}	1.390×10^{-2}	1.060×10^{-2}	$.0119 \pm .0019$	$.0119 \pm .0009$
	92	6.418×10^{-3}	6.184×10^{-3}	1.510×10^{-2}	1.096×10^{-2}	$.0127 \pm .0010$	$.0126 \pm .0001$

σ_B - Born approximation calculation

$\sigma_{Pc}^{\phi o}$ - Øverbo point coulomb calculation (Øo-67)

$\sigma_{Sc}^{\phi o}$ - Øverbo screening corrected calculation (Øo-79)

σ_{Sc}^{TP} - Tseng and Pratt screening corrected calculation (Ts-72)

a - (Øo - 79)

b - (Ts -72)

As seen in fig. 3.18 (a) Experimental σ_x/σ_{Cu} results for Tin and Gold are in very good agreement with calculation of øverbo (øo - 79) at 1.115 Mev. In fig. 3.18 (b) experimental results of Girard et al (Gi - 74) at 1.119 Mev for Tin, lead and Uranium are shown.

Fig. 3.19 shows σ_2/σ_{Cu} according to Born approximation calculation and calculation of øverbo(øo - 79) along with the results of different experiments.

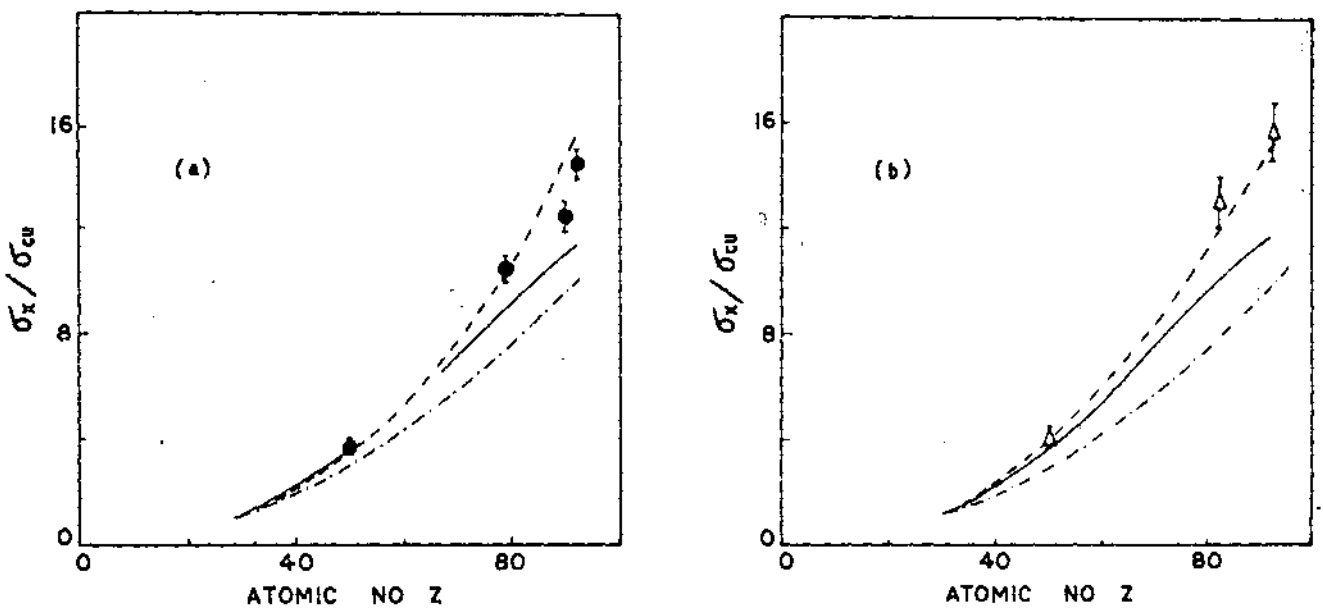

FIG. 3.18. GRAPHS SHOWING σ_x/σ_{cu} Vs Z ACCORDING TO BORN APPROXIMATION (– · – · –). ACCORDING TO REF. (T_s -72) (——) ACCORDING TO REF. (ϕ_0 -79) (– – –) AT 1.115 MeV.

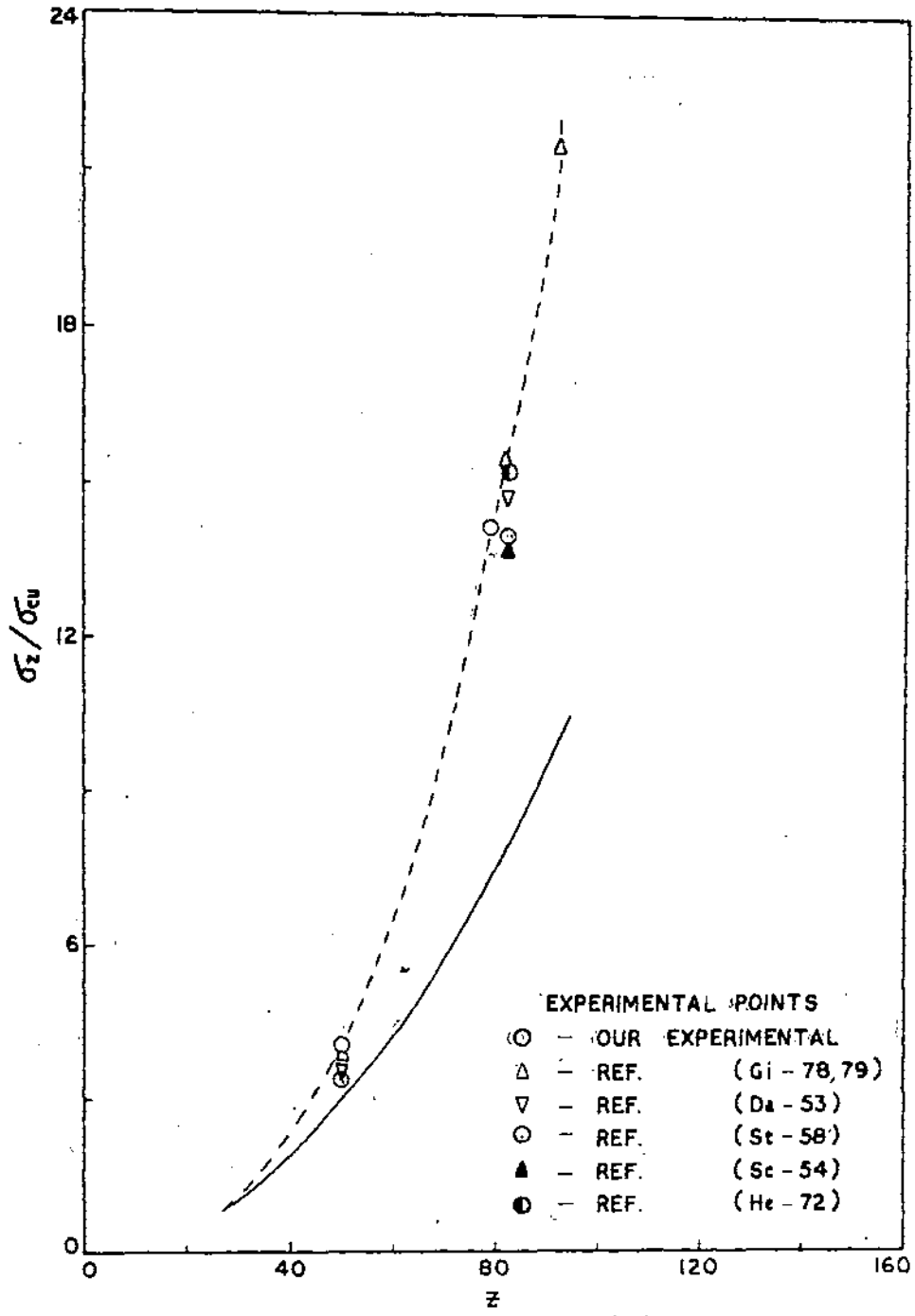

FIG. 3.19. GRAPHS SHOWING σ_Z / σ_{Cu} VS Z ACCORDING TO BORN APPROXIMATION (———), ACCORDING TO SCREENING CORRECTED CALCULATION OF ØVERBO (Øo –79) (– – – – –) AT (1.3325 + 1.1732) MeV.